Deep–Sea Research II 195 (2022) 105012

Contents lists available at ScienceDirect

Deep-Sea Research Part II

journal homepage: www.elsevier.com/locate/dsr2

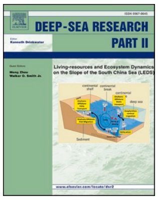

Influence of the 2014–2016 marine heatwave on seasonal zooplankton community structure and abundance in the lower Cook Inlet, Alaska

Caitlin A.E. McKinstry[a,*], Rob W. Campbell[a], Kris Holderied[b]

[a] Prince William Sound Science Center, 300 Breakwater Avenue, Cordova, AK, USA
[b] National Oceanic and Atmospheric Administration, National Ocean Service, Centers for Coastal Ocean Science, Kasitsna Bay Laboratory, 95 Sterling Highway, Suite 2 Homer, AK, USA

ARTICLE INFO

Keywords:
Zooplankton
Community composition
Marine heatwave
Indicator species
Cook inlet
Gulf of Alaska

ABSTRACT

During the 2014–2016 Pacific marine heatwave (MHW), seabird die-offs, declines in forage fish populations, and the appearance of subtropical marine taxa (e.g. ocean sunfish, skipjack tuna) occurred in the northern Gulf of Alaska; however, the response of the zooplankton community to the MHW remains poorly understood. As part of the Gulf Watch Alaska program in Cook Inlet, zooplankton, phytoplankton, and a suite of oceanographic variables were collected monthly from 2012 to 2018. Surface zooplankton were collected via vertical tows (0–50 m) with a 333 μm bongo net along with CTD data and chlorophyll *a* concentration. Generalized additive models showed that seasonal zooplankton abundance peaked mid-June and declined into late January. During the MHW, monthly temperature anomalies ranged from +0.2 to +2.8 °C in 2015 and 2016, but monthly means of large lipid-rich calanoid copepods showed no clear declines in abundance compared to before and after the MHW suggesting that these copepods had some resiliency. An indicator species analysis using 88 of the most common zooplankton taxa produced five groups of zooplankton based on season. A BIO-ENV Best model showed that the environmental variables best explaining the observed zooplankton community structure included SST, temperature of the top 50 m of the water column, mixed layer depth (MLD), MLD temperature, and integrated chl *a* ($\rho = 0.3491$, Mantel Test: $r = 0.3491$, $\alpha < 0.05$). Seasonal transitions of community groups displayed a phenological shift in 2016 when the late spring group of meroplanktonic larvae and the fall group of warm water copepods (WWC) typical of the Northern California Current system appeared earlier and persisted for longer compared to before and after the MHW. WWC abundance increased during the fall seasons of the MHW. Throughout 2015–2016, the elevated abundance of WWC compared to previous years and before/after the MHW suggested that warmer than average oceanographic conditions in the winter of 2015/2016 may have been sufficient to allow for an overwintering population in this area. A potential overwintering population of a warm water predatory copepod, *Corycaeus anglicus*, was observed and may have direct fine scale predator/prey impacts on zooplankton in this region.

1. Introduction

The northern Gulf of Alaska experienced an unprecedented marine heatwave (MHW) between 2013 and 2016. Known colloquially as “The Blob”, this MHW was caused by a reduction in winter heat fluxes driven by a stable atmospheric high pressure system (Bond et al., 2015). In the Gulf of Alaska, the MHW exhibited peak sea surface temperature (SST) anomalies in excess of 3 °C during the 2013/14 winter (Di Lorenzo and Mantua, 2016). The MHW had myriad impacts on the Gulf of Alaska ecosystem, including observations of many taxa more common far to the south (Perry et al., 2017; Brodeur et al., 2017; McKinstry and Campbell, 2018), a die-off of millions of seabirds (Piatt et al., 2020), reductions in the body condition of key forage fishes (von Biela et al., 2019), increases in whale mortality (Savage, 2017) and a recruitment failure and stock collapse in Pacific cod populations (Barbeaux et al., 2019) and forage fish communities (Arimitsu et al., 2021). The impacts of this unprecedented MHW were observed at every trophic level including primary production. In lower Cook Inlet and its Kachemak Bay, harmful algal blooms of the thecate dinoflagellate *Alexandrium cantenella* increased during this time with increasing water temperatures (Vandersea et al., 2018). The effects of the MHW on secondary production among zooplankton in Cook Inlet and Kachemak Bay have not been assessed.

---

* Corresponding author.
E-mail address: cmckinstry@pwssc.org (C.A.E. McKinstry).

https://doi.org/10.1016/j.dsr2.2021.105012
Received 1 March 2021; Received in revised form 23 November 2021; Accepted 30 November 2021

The Gulf Watch Alaska (GWA) long-term monitoring program was established in 2012 to assess the long term environmental changes in the Exxon Valdez Oil Spill and how these changes affect pelagic and near-shore interactions. Through these monitoring efforts, a time series of the biological oceanography of lower Cook Inlet has been collected throughout the MHW disturbance.

As in most high latitude systems, zooplankton are the ecological driver of the marine ecosystems they inhabit by forming the link between primary production by phytoplankton and upper trophic level predators including marine mammals, seabirds, and economically important fishes. The current documented outcomes of MHWs on zooplankton communities have varied between few significant changes to large phenological and abundance based effects making the results of these disturbances challenging to predict. During the 2012 MHW in the Northwest Atlantic, the copepod *Calanus finmarchicus*; a key prey species for the region and the critically endangered North Atlantic Right Whale, did not decline in abundance but produced the largest spring cohort during an eight year study after the end of the MHW (Runge et al., 2015). In contrast, the Tasman Sea 2015/2016 MHW resulted in significantly lower peak abundances of zooplankton, a phenological

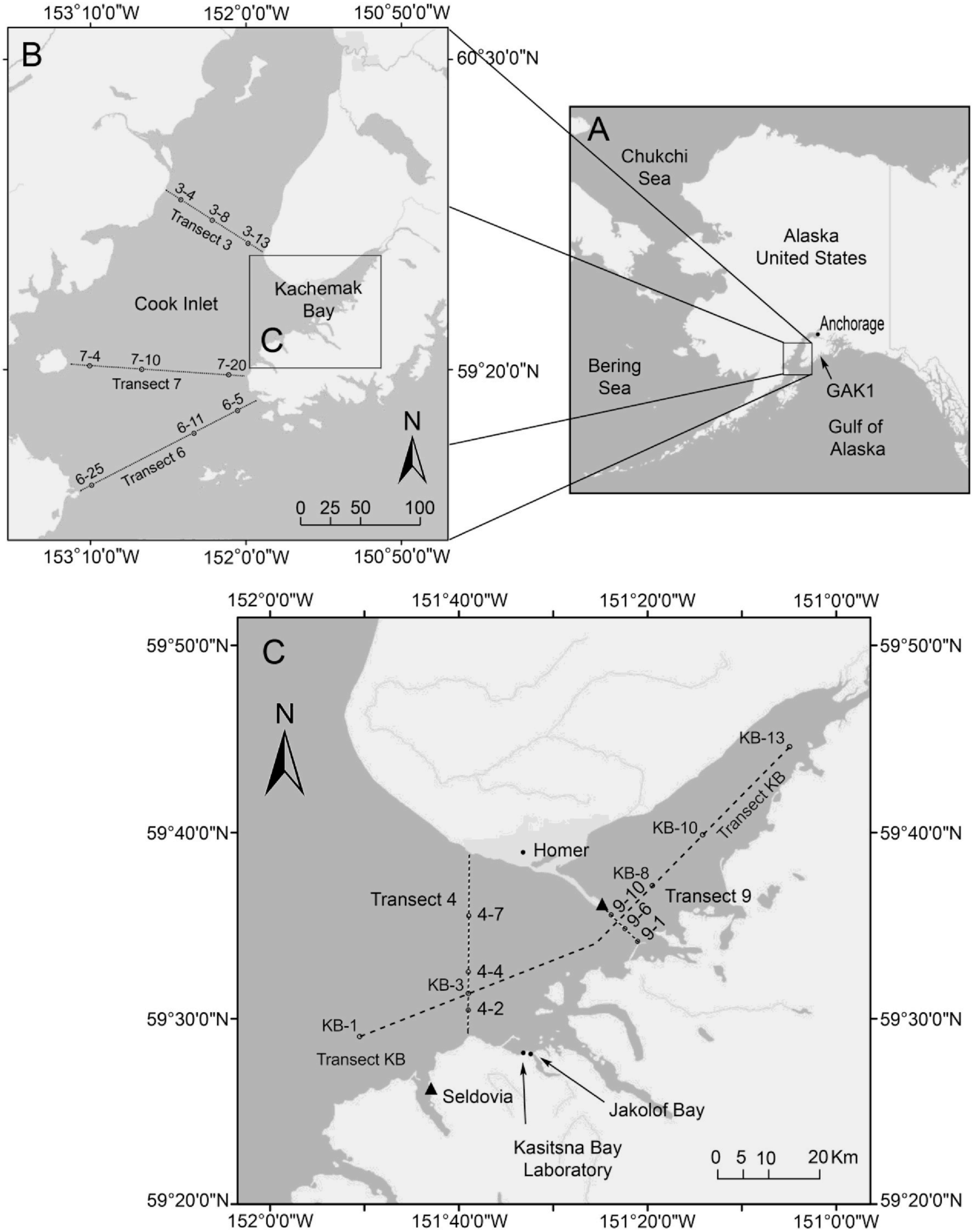

Fig. 1. Map of the study region including lower Cook Inlet (B) and Kachemak Bay (C) with transects (dashed lines) and stations (open circles) along each transect. Modified with permission from Vandersea et al. (2018).

shift of this abundance to later in the summer, and an increase in warm water associated copepod species (Evans et al., 2020). The latter pattern was also observed off the coasts of Oregon, Washington, and Vancouver during the Pacific MHW (Peterson et al., 2017; Fisher et al., 2020; Hipfner et al., 2020). In the fjord system of Prince William Sound (PWS), zooplankton communities also showed distinct shifts in species composition during the Pacific MHW, most notably in the increased abundance of six species of warm water copepods (WWC) more commonly associated with the Northern California Current (NCC) and offshore pelagic regions of the Oregon and Washington coasts (McKinstry and Campbell, 2018).

Cook Inlet (Fig. 1) is approximately 375 km from PWS and is located downstream from PWS in regards to the Alaska Coastal Current (ACC), a geostrophically- and freshwater-driven along-shore current that runs north and westward from the Columbia River along the northern Gulf of Alaska coast. With an immense semidiurnal tidal range (>8m maximum), Cook Inlet and Kachemak Bay experience dynamic circulation patterns driven by fortnightly tides, seasonal freshwater inputs from rain, snow, and glacial melt, and varying incursions of ACC waters from the Gulf of Alaska (Okkonen et al., 2009; Johnson, 2021). The bathymetry of Cook Inlet is relatively shallow for the Gulf of Alaska, with channels of less than 200 m depth located on the southeast corner of the inlet running into Kachemak Bay (~175 m maximum depth) and at the southwest side of the inlet entrance (~185 m maximum depth).

1.1. *Statement of the problem*

Here we present evidence of how the 2014–2016 Gulf of Alaska MHW affected the zooplankton community in Cook Inlet and Kachemak Bay from analyses of data collected before, during, and after the prolonged heat wave. Through data collected for the GWA long-term monitoring program, zooplankton from the region were analyzed in this study to understand 1) the spatial and temporal variability of zooplankton species in this region using generalized additive models and monthly mean abundance estimates, and 2) the community structure of zooplankton associated with the nearshore marine system via indicator species analysis and multivariate ordination techniques. These data represent the first seven years (2012–2018) of GWA zooplankton sampling in lower Cook Inlet and Kachemak Bay.

2. Materials and methods

2.1. *Field collection*

Zooplankton and oceanographic data were collected from multiple stations across three transects in lower Cook Inlet and three transects in Kachemak Bay (Fig. 1) during daylight and nighttime hours; the stations and transects were chosen to extend and expand an oceanographic time series from earlier monitoring efforts following Okkonen et al. (2009). Three transects in lower Cook Inlet (Transects 3, 6, 7) were sampled quarterly between 2012 and 2016 and on the eastern sides of the transects in 2017 and 2018. Two cross-bay transects in Kachemak Bay were sampled quarterly (Transect 4) or monthly (Transect 9) between 2012 and 2018 and a third, along-bay transect from the entrance to the head of the bay was added in 2017 (Transect KB).

At each station, a vertical cast was obtained with a Sea-Bird Electronics model SBE 19plus V2 (Bellevue, Washington, USA) conductivity-temperature vs depth profiler (CTD), lowered from surface to bottom at approximately 1 m/s descent rate. Ancillary sensors integrated with the CTD included a combined fluorometer/turbidity sensor (WET Labs ECO-FL-NT), an underwater photosynthetically available radiation (PAR) sensor (Li-Cor LI-192 PAR) and a dissolved oxygen sensor (SBE 43F). Each oceanographic cast was processed with standard Sea-Bird Electronics data processing software routines. Temperature, salinity, density and ancillary data were binned in 1-m depth intervals. A number of statistics were computed from each cast, including sea surface temperature (SST; 0–1 m), sea surface salinity (SSS), mixed layer depth (MLD), mean temperature of the mixed layer (TML), mean salinity of the ML (SML), and mean temperature and salinity in the top 50 m (or to bottom, if shallower). The MLD was calculated according to the method of Musgrave et al. (2013) with a density threshold of 0.125 kg m^{-3}. The maximum chlorophyll-*a* (chl *a*) and depth of the chlorophyll maximum were computed from the CTD fluorometer data profile, and integrated chl *a* in the top 50 m (or to bottom) was calculated using the trapezoid rule. SST anomalies were calculated as the residual to a second order cosine curve fit to data from all years to remove seasonality (Campbell 2018).

Zooplankton net tows (n = 489) were carried out with a 0.6 m diameter bongo net with 333 μm mesh size, towed vertically from 50 m (or near bottom) to the surface during daylight and sometimes nighttime hours. Zooplankton were preserved in 5% formalin solution for later enumeration. Processing and analysis of zooplankton samples followed McKinstry and Campbell (2018). Briefly, samples were subsampled with a Folsom splitter until at least 200 individuals of the most numerous taxa were present. Samples were then counted for species composition. Less abundant macrozooplankton (e.g. euphausiids, ichthyoplankton) were enumerated in higher fraction aliquots. For many of the zooplankton samples collected during winter months, which had lower abundances, the sample was not subsampled, and zooplankton were enumerated from the entire tow. For all analyses, *Neocalanus plumchrus* and *N. flemingeri* were aggregated as one genus: *Neocalanus* spp.

2.2. *Statistical analyses*

Statistical analysis of zooplankton trends were analyzed using the statistical package R (R Core Team, 2019). To stabilize the typically high variance of zooplankton abundance, data were log transformed by $\log_{10}(n+1)$ (Keister and Peterson, 2003). Seasonal abundance cycles were produced using generalized additive models (GAM) based on a Gausian distribution and identity link function with day of the year as the explanatory variable (McKinstry and Campbell, 2018; Wood, 2004). GAMS were used as an illustrative exercise to display the broad seasonal abundance patterns of zooplankton groups.

After a previous version of these analyses displayed uniformity of species groups based on transect and station (Doroff et al., 2016), stations along each transect during a cruise were combined and averaged for multivariate analyses (n = 196 transects). A hierarchical clustering analysis (HCA; R base package) using Ward's agglomerative method with Euclidean distances was used to produce pairwise groupings of similar tows based on abundance of species present in each transect (Manley, 1994). The pairwise site groupings were further analyzed to identify the taxa driving this pattern using an indicator species analysis (ISA; R package: "indicspecies"; De Caceres and Legendre, 2009).

Indicator species were identified statistically using the ISA method developed by Dufrene and Legendre (1997). Indicator species are indicative of an HCA group based on abundance and frequency of occurrence within an HCA group and are given an indicator species value between 0 and 1. A single species observed at a single site cannot represent a group comprised of many sites and would therefore have a very low ISV (Bakker, 2008). At the same time, abundant species found frequently in all groups would also result in a low ISV. Indicator species with high ISVs occur abundantly within a single group. Both the original authors of the ISA and authors using this method with zooplankton data (Morgan et al., 2003; Peterson and Keister, 2003; Keister et al., 2003; Keister et al., 2011) highlighted the usefulness of a species presence threshold to reduce the importance of itinerant species. Based on these studies and our averaging of stations across transects, we omitted rare taxa that were present in <6.5% of transects.

Non-metric multidimensional scaling (NMDS) with a Bray-Curtis dissimilarity matrix was employed to confirm the HCA and ISA clustering of zooplankton community structure based on abundance. The most appropriate dimensions, 2D, 3D, and 4D plots, were calculated.

The plot with the lowest stress was included in the results. Oceanographic variables were compared to the NMDS results with a BIO-Env Best model (Clarke and Ainsworth, 1993; R package: "vegan"; Oksanen et al., 2019). This test assessed what set of oceanographic variables best explained the spatial ordination of zooplankton samples presented by the NMDS. To test the significance of the BIO-ENV Best correlations, a Mantel test based on the Spearman's rank correlation coefficient was used ($\alpha < 0.05$).

3. Results

3.1. Oceanography

SST anomalies showed the MHW began to affect lower Cook Inlet and Kachemak Bay early in 2014, with strong warm (positive) anomalies present by summer of 2014 and the largest positive anomalies observed in the summer of 2015 (Fig. 2). The MHW persisted into 2016 when water temperatures remained elevated relative to seasonal norms throughout the entire year. In the late fall of 2016, temperature anomalies began to decline across the Gulf of Alaska and in Cook Inlet/Kachemak Bay, signaling the termination of the MHW. MLD fluctuated seasonally with a minimum MLD ($<$5m) in summer and maximums during the winter (Fig. 2, middle panel). Integrated chl *a* peaked in spring (May–June) then declined into summer and fall (Fig. 2, bottom panel). A second chl *a* peak occurred in the fall in some years (particularly 2016), but not all, and the seasonal chl *a* average showed only a very small fall peak overall.

3.2. Zooplankton abundance

Microscopic analysis identified 237 unique zooplankton species and categories (Supplemental Table 1). The largest taxonomic group was calanoid copepods, accounting for 57 (24%) of the taxa identified. For the below analyses, 88 species of common zooplankton species were selected based on their presence in 93.5% of plankton tows.

Seasonal trends of zooplankton abundance as illustrated by GAMs (Fig. 3A) depicted a general trend of low abundance in the winter ($>$100 ind. m^{-3}) followed by a sharp increase coinciding with the increase in integrated chl *a*. The overall peak abundance of zooplankton occurred in late spring/early summer (1683 no. m^{-3} [95% CI: 1150–2187]) driven by a high abundance of small copepods ($<$2 mm). Throughout the summer and fall, zooplankton abundance gradually declined with no clear peaks in late fall to indicate the consistent occurrence of a fall bloom of secondary productivity. Large calanoid copepod abundance quickly peaked (74 no. m^{-3} [95% CI: 55–97]) in early spring and displayed a steady decline through summer and into fall (Fig. 3).

A number of copepod taxa common to the California Current (Morgan et al., 2003; Peterson et al., 2017; McKinstry and Campbell, 2018; Suryan et al., 2021) were identified in our Alaskan samples; these "warm water copepods" (WWC) included *Calanus pacificus*, *Clausocalanus* sp. *Ctenocalanus vanus*, *Corycaeus anglicus*, *Mesocalanus tenuicornis*, and *Paracalanus parvus*. WWC abundance remained consistently low ($<$10

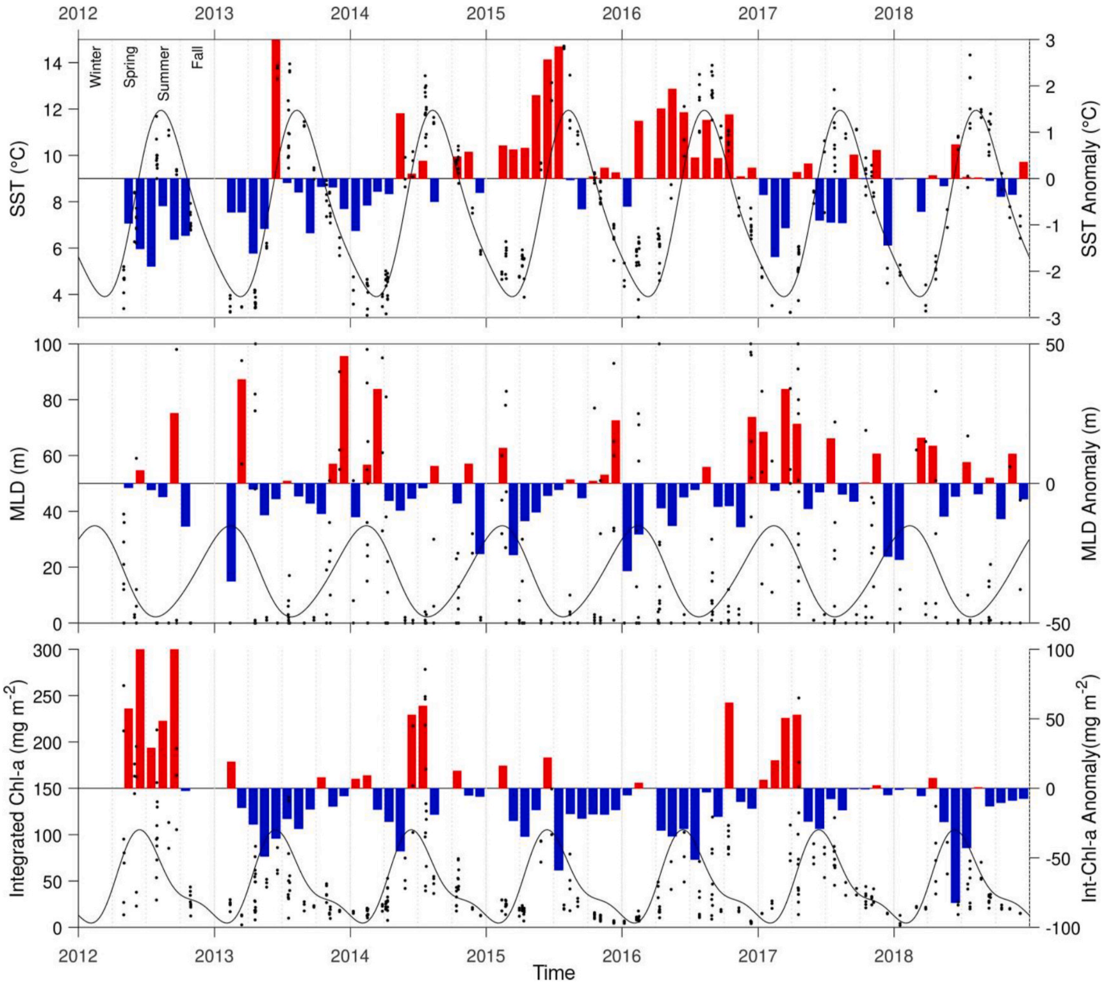

Fig. 2. Time series of oceanographic variables found significant by the BIO-ENV "Best" model. Sea surface temperature anomalies are represented as red (positive) and blue (negative) bars. Dots indicated data points. Trend lines were calculated for mean annual cycles per each variable as indicated by solid lines. Gray grid lines indicate the beginning of seasons.

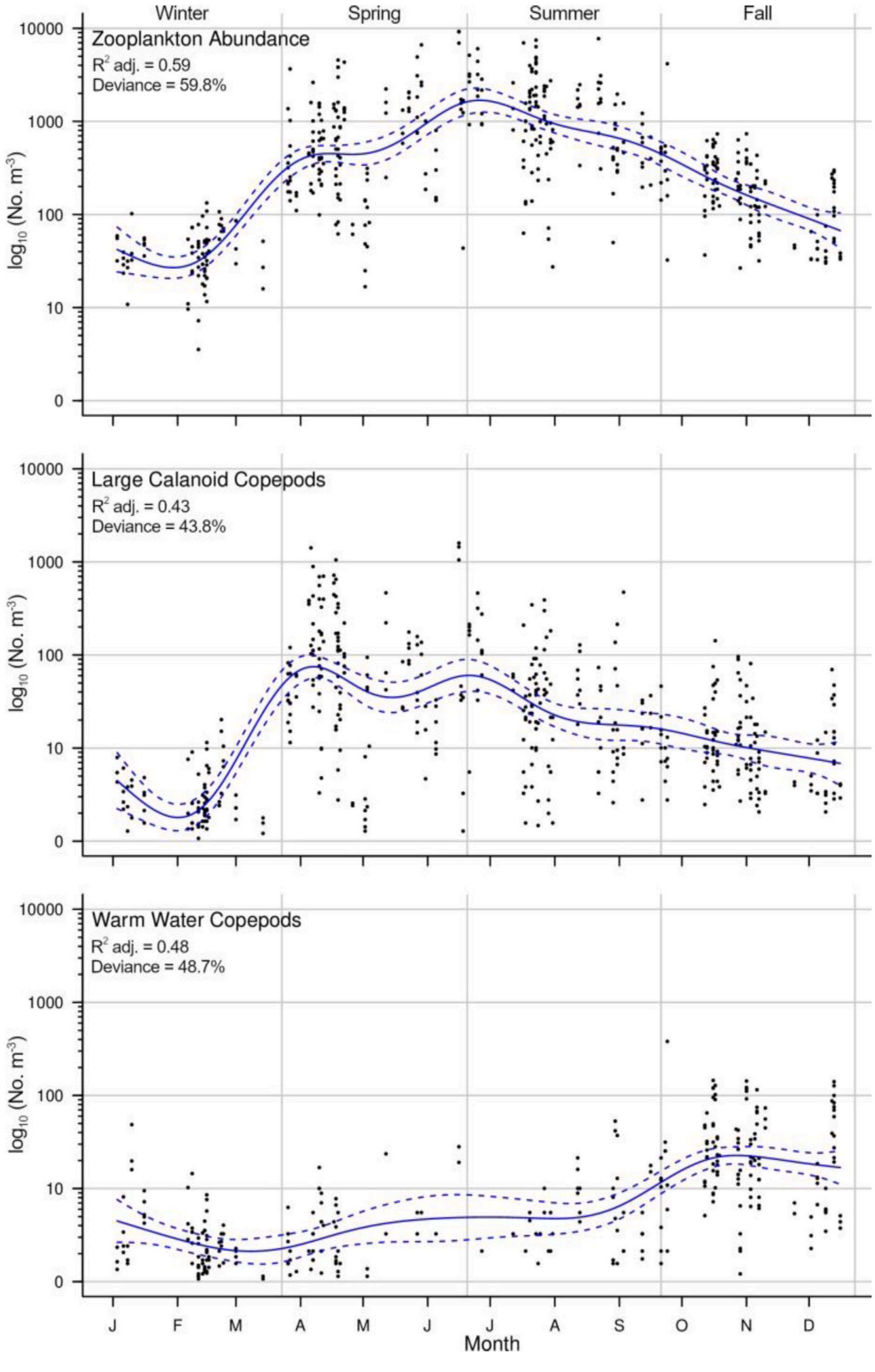

Fig. 3. General trends in seasonal abundance of corresponding zooplankton categories as $\log_{10}(n+1)$; (•) indicate observations for overall zooplankton, large calanoid copepods (>3 mm), and warm water copepods (WWC) common along the coast of California to Washington. Gray grid lines indicate seasons. Seasonal abundance patterns of zooplankton in Cook Inlet and Kachemak Bay with GAM best-fit models (—) and 95% confidence intervals (- -). WWC include *Calanus pacificus*, *Clausocalanus* spp., *Ctenocalanus vanus*, *Corycaeus anglicus*, *Mesocalanus tenuicornis*, and *Paracalanus parvus*. Large calanoid abundance combines *Calanus marshallae*, *Epilabidocera longipedata*, *Eucalanus bungii*, *Metridia okhotensis*, *M. pacifica*, *Neocalanus cristatus*, *N. plumchrus*, and *N. flemingeri*.

no. m^{-3}) throughout the spring and summer then peaked in the fall (22 no. m^{-3} [CI: 17–7]). Abundance during the winter months sharply fell.

Yearly seasonal cycles of overall monthly mean abundance and copepod groups (Fig. 4) generally followed the GAM seasonal trends between years except for WWC during the MHW. In the fall of 2014, WWC displayed the highest abundance (380 no. m^{-3}; n = 1) during the study period, which was an order of magnitude higher than previous years (2012: 9 ± 8 no. m^{-3}, 2013: 31 ± 11 no. m^{-3}). In the winter of 2015/2016, WWC abundance departed from the average seasonal cycle (as depicted by the GAM). Instead of a rapidly declining in abundance during the winter as in past years, these copepods were present throughout the winter 2015/2016 months then slowly increased in abundance from spring 2016 to summer peaking in the fall. In 2018, WWC were entirely absent from spring through late summer, appearing again only in the fall (September).

3.3. Zooplankton community structure

The HCA (cophenetic correlation coefficient = 0.514) produced five clusters of transects (Supplemental Fig. 1) based on a clear seasonal progression of species composition. Of the 88 species and categories of zooplankton included in the ISA, 75 were identified as significant

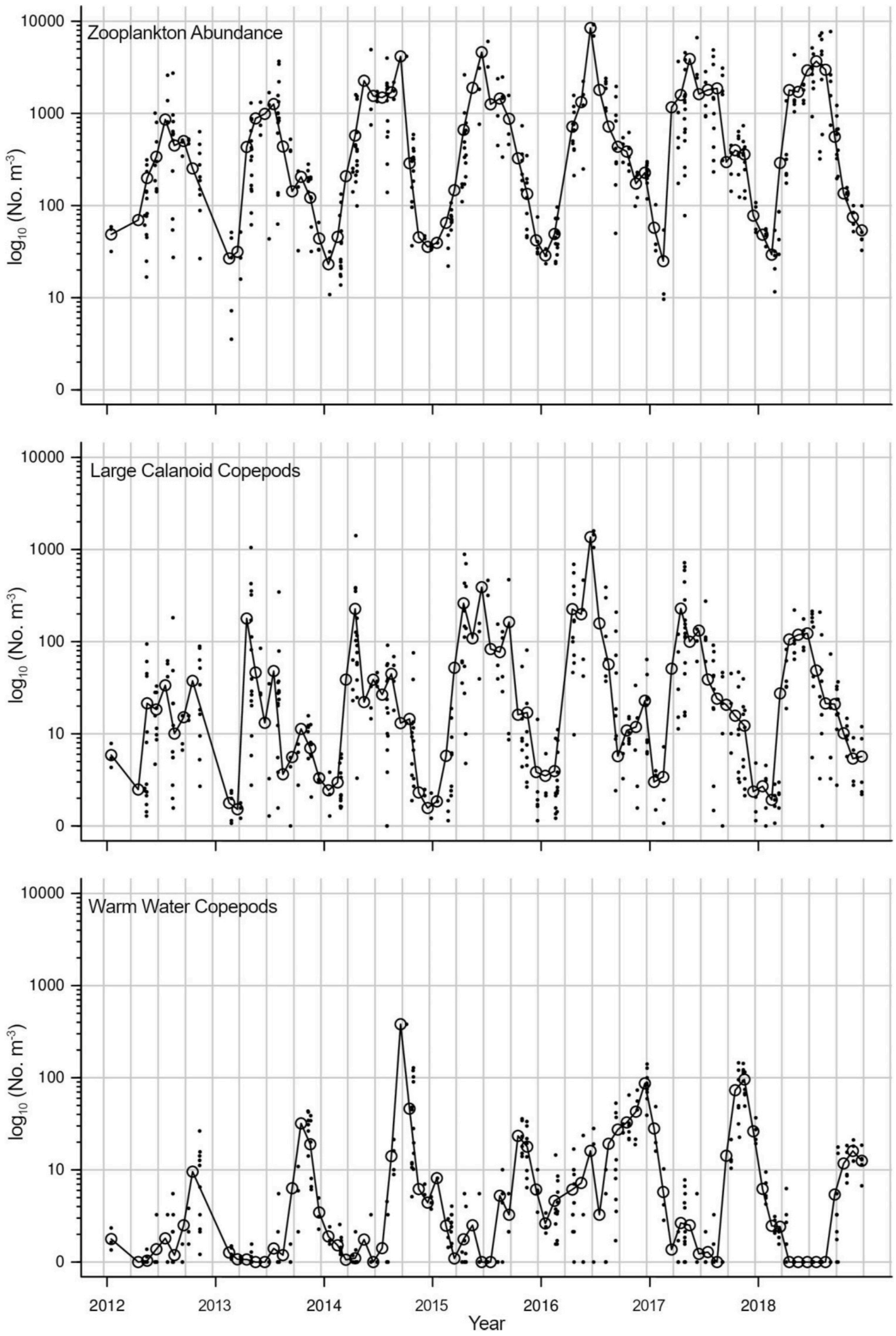

Fig. 4. Monthly means time series of zooplankton during the study period of corresponding zooplankton categories as $\log_{10}(n+1)$; (•) indicate observations for overall zooplankton, large calanoid copepods (>3 mm), and warm water copepods (WWC) common along the coast of California to Washington. Gray grid lines indicate seasons. Note that standard deviation is not included and variance should be expected. The (○) represent monthly means (n = 78). Species categories are defined as in Fig. 3.

indicator species ($\alpha < 0.05$; Fig. 5A). ISV ranged from 0.31 (ichthyoplankton) to 0.84 (*Pleurobrachia*). A higher ISV denotes good indicator species for the group. These indicator species are less likely to be found in any of the other groups.

From the ISV (Fig. 5B), a uniform winter assemblage appeared in both Kachemak Bay and Cook Inlet; this group included five copepods (one warm water copepod: *Ctenocalanus vanus*). An early spring group reliably emerged by late March defined by forage fish ichthyoplankton and several large calanoid copepods including all species of *Neocalanus*. After the end of the spring bloom and decline in integrated chl *a* (Fig. 2), large calanoid copepod abundance quickly declined (Fig. 3) as well. The early spring group then gave way to a distinct late spring group comprised of mainly meroplanktonic larvae. The late spring group occurred mainly in Kachemak Bay, appearing once in Cook Inlet in 2017 (Fig. 4). After a transition period in June, the late spring group dissipated and was replaced by the summer group. The summer group was defined by a small number of meroplankton, the small calanoid copepod *Acartia longiremis* and gelatinous zooplankton. The ISA grouped five of the six WWC species observed in the Cook Inlet region into the Fall group along with several gelatinous zooplankton and copepods that remain active in the water column throughout the year, e.g. *Oithona* spp. Half of the WWC (*Paracalanus parvus*, *Mesocalanus tenuicornis*, *Corycaeus*

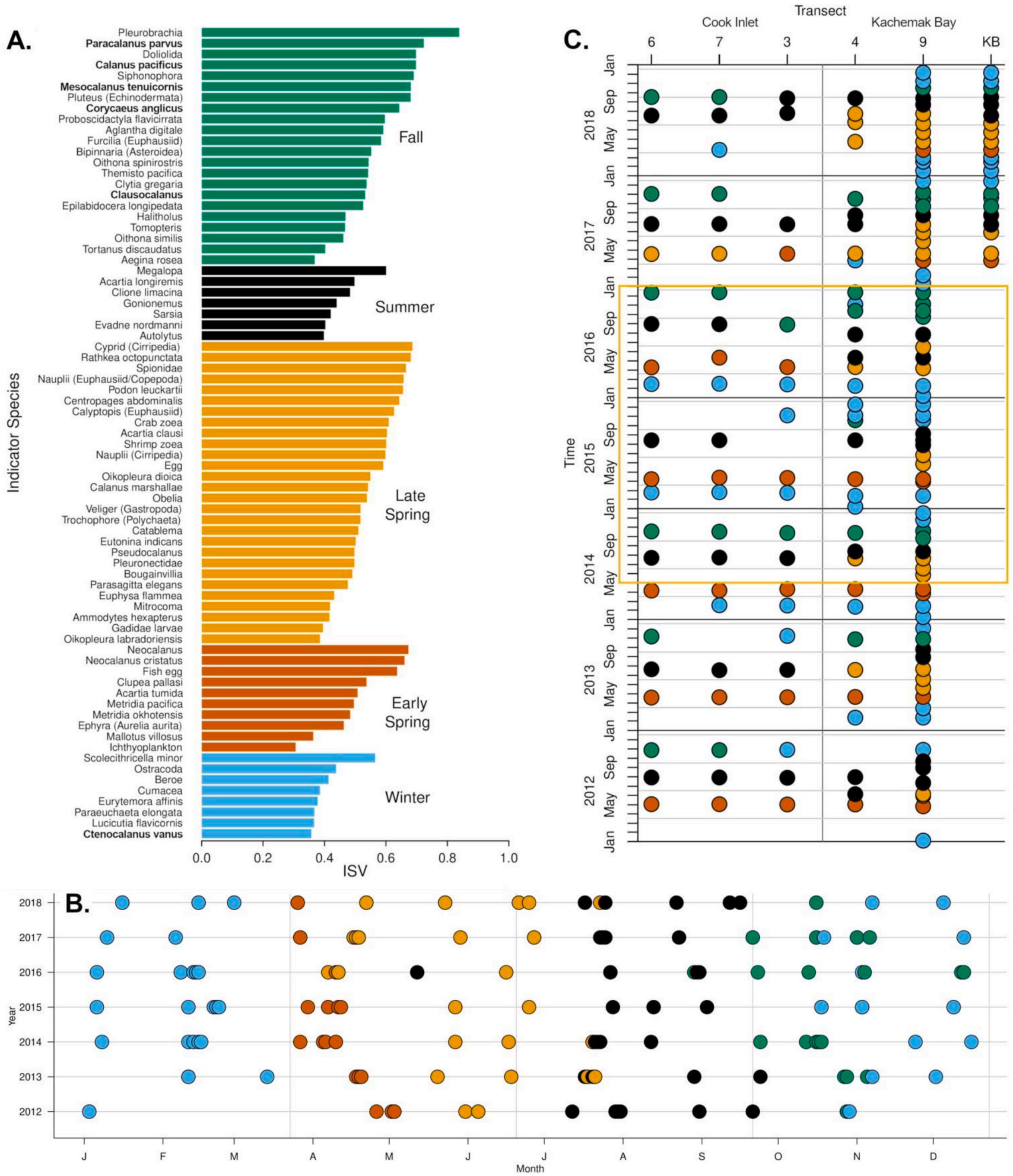

Fig. 5. **A.** Indicator species values (ISV) that defined each group of the hierarchical clustering analysis. Of the 88 species/categories included in the analysis, the 74 most significant ($p < 0.05$) are presented. Warm water copepod species are in **bold**. **B**. Indicator species analysis (ISA) groups based on year and day of year to show seasonal transition of communities (all transects combined). Colors correspond to the indicator species group of each tow (see panel **A.**). Gray grid lines indicate seasons. **C.** Spatial scatter plot of time and ISA groups in each transect ($n = 196$). The gray vertical lines indicate seasons while the marigold box defines the duration of the marine heatwave in Cook Inlet and Kachemak Bay.

anglicus) were in the 90th ISV percentile (>0.64) with *Paracalnus parvus* showing the second highest ISV (0.67) for all statistically significant indicator zooplankton ($n = 75$). The fall group emerged early in the season (late September) and persisted only into late October/early November.

During and after the appearance of the MHW, inter-annual variation in the timing and duration of ISA groups became apparent (Fig. 5C). In 2016, the early spring zooplankton community appeared only in Cook Inlet and was seemingly replaced with the late spring group in Kachemak Bay. The late spring group's appearance in early April of 2016 was the earliest during the study period. The summer group usually observed in July–September also appeared earlier than any other time in May at both transects sampled in Kachemak Bay. During the summer months, the fall group appeared as early as late August and persisted into December. The subsequent 2017 early spring group was absent from most of Cook Inlet. The late spring community again appeared earlier in Kachemak Bay and for the first time was present in Cook Inlet.

The NMDS further showed that ISA groups clustered together with overlap appearing among subsequent seasonal groups. The dimensionality with the lowest stress values for the NMDS ordination

(Supplemental Fig. 2) was 4D (stress: 0.088) compared to 2D (0.182) and 3D (0.116). NMDS confirmed the seasonality of groups displayed in the HCA pairwise comparison and showed the general relationships among transects shown in the ISA groupings. The BIO-ENV Best model of oceanographic variables selected SST ($\rho = 0.3246$), mean temperature in the top 50m of the water column ($\rho = 0.0075$), TML ($\rho = 0.0078$), MLD ($\rho = 0.0058$), and integrated chl *a* ($\rho = 0.0034$) as the variables that cumulatively ($\rho = 0.3491$) showed the highest positive correlation (Mantel Test: $r = 0.3491$, $\alpha < 0.05$) to the NMDS ordination.

4. Discussion

Using several different statistical approaches, a consistent seasonal progression of zooplankton abundance and community composition emerged throughout the year in lower Cook Inlet and Kachemak Bay and coincided with seasonal changes in temperature. These results are in line with and add to the observations by others (Batten et al., 2018; McKinstry and Campbell, 2018; Arimitsu et al., 2021; Ashlock et al., 2021; Suryan et al., 2021) in regard to of oceanographic and zooplankton community changes resulting from the 2014–2016 MHW in the Northeastern Pacific. Community structure and phenology of zooplankton in this region was strongly influenced by all oceanographic variables associated with seawater temperature. During the MHW, when SST was consistently more than +0.5 °C warmer than average, the timing of the seasonal transitions of zooplankton communities was disrupted. This was especially so in 2016 when both the spring and fall communities appeared earlier and persisted for longer compared to before and after the MHW. Warm water copepod abundance increased during this time during the fall and even persisted through the winter of 2016 (Fig. 4). GAMs of the seasonal cycle in zooplankton abundance (Fig. 3) had similar patterns to those produced from Prince William Sound GWA data (McKinstry and Campbell, 2018); zooplankton sampling, analysis, and the time frame were similar to the present study. The complex changes to the zooplankton community caused by the MHW described here may have contributed to bottom-up related effects that resulted in unprecedented die-offs (i.e. common murres) and trophic shifts reported in the Northern Gulf of Alaska region.

The timing of peak abundance for all zooplankton was days to weeks earlier in Cook Inlet and Kachemak Bay (mid-June) than in PWS (early July). In the case of large calanoid copepods, peak abundance occurred months earlier in the spring in Cook Inlet and Kachemak Bay (beginning of April) than PWS (beginning of June). The Cook Inlet region is characterized by relatively shallow bathymetry and a large tidal range compared to the enclosed deep fjords characteristic of PWS. Tidal mixing, along with freshwater inputs from many glacial rivers, increases turbidity (Environment and Natural Resources Institute (ENRI), 1995) in Cook Inlet waters, especially from snow and glacier melt from spring to late summer (Okkonen et al., 2009), causing a limited and short lived primary productivity season (Vandersea et al., 2018). In only two years of this study (2012 and 2014) did integrated chl *a* reach levels comparable to those observed in PWS during the spring (>200 mg m^{-2}). This may explain the rapid decline of large calanoid copepods after the initial spring peak.

The relative spatial uniformity of zooplankton communities in Cook Inlet and Kachemak Bay as shown by the ISA (Fig. 5C) significantly deviated only during spring and may have been driven by transport differences between Cook Inlet and Kachemak Bay. The early spring community, found more often in Cook Inlet rather than Kachemak Bay sampling sites, was described by the presence of large calanoid copepods (*Neocalanus cristatus, N. plumchrus/flemingeri*) characteristic of those observed on the adjacent shelf (Coyle and Pinchuk, 2005; Sousa et al., 2016; Batten et al., 2018). Lower Cook Inlet experiences more daily tidal flushing and is connected to the northern Gulf of Alaska shelf and ACC, than is the shallower Kachemak Bay estuary (Johnson, 2021). The species composition of the zooplankton community in the more protected Kachemak Bay was comprised of more larval meroplankton taxa (e.g. barnacle, polychaete, ichthyoplankton) indicative of estuarine conditions in the late spring. The disappearance of larval meroplankton from the water column, presumably after settling to the bottom or transport out of the area, signified the transition from the late spring to the summer zooplankton community.

Overall zooplankton and large calanoid copepod abundance from 2012 to 2018 did not show clear associations with the appearance and dissipation of the MHW. In 2016, when positive SST anomalies were sustained throughout the year and when the warmest winter and spring months occurred, both overall zooplankton (8450.22 ± 1317.67 no. m^{-3}) and large calanoid copepods (1362.92 ± 1237.71 no. m^{-3}) reached the highest monthly means recorded here. Integrated chl *a* did not appear elevated in spring 2016, indicating that phytoplankton biomass was not above average. This may indicate these copepods have some resiliency to warmer waters, or that, although surface waters were warmer than average, they did not approach the thermal maximum for those species (the thermal range of the taxa of the northern GoA is not well described). This is in contrast to many documented effects of MHWs on zooplankton communities elsewhere. Off the eastern coast of Tasmania during the 2015/16 Tasman Sea MHW, common cold water copepod abundance was 43% lower compared to normal years (Evans et al., 2020). During the Pacific MHW, off the coast of Vancouver Island and OR, a clear inverse pattern of abundance was also observed in cold water associated copepods (including *Calanus marshallae*, *Eucalanus bungii*, *Neocalanus cristatus*, and *N. plumchrus*; Peterson et al., 2017). More generally, reductions in cold water associated copepods tend to occur during warmer stanzas in the GoA associated with positive phases of the Pacific Decadal Oscillation basin wide index of surface (Di Lorenzo and Mantua, 2016; Peterson et al., 2017; Hipfner et al., 2020). Under PDO neutral conditions, wind and net ocean transport of cold water copepods from the North Pacific flow southward in the summer then switches to a northward transport of warm water copepods from the California Current system in the winter (Peterson et al., 2017). During the Pacific MHW, when PDO conditions were positive, southward currents weakened and a strengthening of poleward currents prevented southward transport of cold water copepods (Peterson et al., 2017; Fisher et al., 2020). Zooplankton abundance from the Alaskan Shelf, collected via continuous plankton recorders (CPR), also did not display a decline in large calanoid copepod abundance during the MHW (Batten et al., 2018) further suggesting that the transport mechanisms experienced further south do not immediately impact large calanoid copepods in Kachemak Bay and Cook Inlet.

WWC showed clear changes in abundance coinciding with the MHW possibly indicating an incursion of water masses from the south. Before 2014, WWC abundance peaked in the fall, with a few dozen or less individuals per cubic meter (Fig. 4; Oct. 2012: 8.56 ± 8.05 no. m^{-3}, Oct. 2013: 30.95 ± 10.91 no. m^{-3}). In 2014, WWC abundance quickly increased, with the highest observed abundance in September of that year (379.93 no. m^{-3}; $n = 1$) representing an order of magnitude increase from previous years. In the fall of 2015, abundance estimates of WWC were again lower (Oct. 22.39 ± 9.61 no. m^{-3}), but were persistently observed at low abundances (<10 no. m^{-3}) late into the 2015/2016 winter compared to the almost undetectable amounts seen in other years suggesting a successful overwintering period. Then, through the spring and summer of 2016, WWC displayed a gradual increase to a peak in the fall. The April–August 2016 period experienced the highest monthly averages for this group especially from 2015 to 2016. The zooplankton communities in the Northern California Current region (Peterson et al., 2017), the Alaskan Shelf (Batten et al., 2018), and PWS (McKinstry and Campbell, 2018) also experienced significant increases in WWC during this time. The North Pacific Current (NPC), the North Pacific basin-wide ocean gyre, was stronger into GoA during the MHW (Fisher et al., 2020) enhancing the teleconnections between the north Pacific transition zone and northern GoA. The appearance of WWC on the Alaskan Shelf, PWS, Cook Inlet, and Kachemak Bay following the MHW indicates that this transport mechanism may reach as far north as the northern Gulf of Alaska via the ACC as suggested by Batten and Walne (2011) during positive PDO cycles.

The presence and timing of WWC indicates warm water masses may have been transported into the nearshore regions of Cook Inlet and Kachemak Bay mainly during the fall season. However, the steady rate of increasing WWC abundance throughout spring-fall 2016 may suggest the persistence of a local population brought to the area during the relatively warm winter 2015/2016. Field and laboratory experiments with individual species of WWC show that these copepods can develop and reproduce in water temperatures similar to those experienced in the late fall and winter during the MHW. However, development to adult stages is longer at these cooler temperatures. *Corycaeus anglicus* can produce three generations of copepods in as little as four months with a declining fall temperature range of 16–12 °C (Digby, 1950). Between 200 and 300 individuals produced over 40,000 individuals after 50 d in an *in situ* mesocosm experiment in Saanich Inlet, BC (Gibson and Grice, 1978). *Paracalanus* produced six generations within nine months (Digby, 1950) and had a development rate of 44 d in 9.7 °C seawater (Liang and Uye, 1996). *Calanus pacificus* has been shown to develop from egg to adult in 26 d at 11.4 °C (Huntley and Brooks, 1982). MHW driven current changes would have had to advect a steady and increasing supply of WWC to Cook Inlet and Kachemak Bay for the duration of 2016 to account for the patterns observed here. Stronger than average poleward warm currents were seen off the coast of OR in the winter of 2015/2016, but these conditions returned to the relatively normal state of net transport switching equatorward in the summer of 2016 (Peterson et al., 2017). Locations such as the partially protected inshore estuarine environment of Kachemak Bay may act as refugia for these copepods and allow a small persistent population to respond quickly to optimal growth conditions like those produced during the MHW. This is opposed to offshore locations (ex: Northern California Current, Alaska Shelf) where WWC abundance has been dictated by water mass transport dynamics affected by the MHW and changes in the NPC (Fisher et al., 2020).

As the global trend in MHWs leans toward higher frequency and increased duration of events (Oliver et al., 2018), assessing the effects on the zooplankton community will allow for a better understanding of trophic changes further up the food web. The energy content of the prey field available to zooplanktivorous predators may decline based on the increased number of WWC and the physiological effects warmer than average conditions have on large calanoid copepods. The suite of WWC observed here were made up of smaller relatively lipid-poor copepods compared to the high energy lipid-rich *Calanus marshallae*, and *Neocalanus* spp. resident to this region. A decline in lipid-rich copepods and an increase in lipid-poor copepods may have contributed to the drop in quality and abundance of zooplanktivorous forage fishes in PWS during the MHW (Arimitsu et al., 2021) possibly exacerbating the massive die-off and reproductive failure of common murres (*Uria aalgae*) in the region (Piatt et al., 2020). The community changes in zooplankton during the MHW presented here in Cook Inlet and Kachemak Bay may have also contributed to this trophic interruption by affecting forage fishes.

Our understanding of how MHWs affect the physiology of large lipid-rich copepods in their ability to collect and retain lipids on an individual species basis is also limited. MHWs may reduce the size and energy content of individual copepods especially during the overwintering diapause phase of the copepod life cycle due to heat-induced increases in metabolism (Campbell et al., 2001). This may affect individual copepod species in the North Pacific with different life histories such as the longer-lived *Neocalanus plumchrus*, which has shown declines in abundance and earlier appearance in surface waters during the warmer than average SSTs created by “The Blob” (Ashlock et al., 2021). There is also a need to look at individual species specific patterns. Here, we analyzed several species of large calanoid copepods as a single group. Ashlock et al. (2021) provides evidence that it is also important to assess specific ecologically significant copepod species to understand the impacts of MHW.

Fine scale predator/prey interactions within the zooplankton community could be affected as well through MHW induced range shifts of copepod predators. For example, the predaceous WWC *Corycaeus anglicus* feeds on small copepod species (e.g. *Pseudocalanus* spp., *Acartia* spp.) and early stages of larger copepods (Landry et al., 1985). *C. anglicus* was not observed in the study region prior to the start of the MHW, but first appeared in early 2014. At peak abundance in the fall of 2017, *C. anglicus* accounted for over 20% of zooplankton (76.45 ± 26.82 no. m^{-3}) recorded in November 2017 and in one tow, 60% of the zooplankton. While it would potentially require numerous and persistent populations of these predators in Cook Inlet and Kachemak Bay, the impacts on the interspecies dynamics of the zooplankton community are difficult to predict with our current understanding. Laboratory experiments have shown that an adult male *C. anglicus* can kill 1.4 small copepods per day (Landry et al., 1985). In the November 2017 instance, this translates to an average of 107.03 ± 37.55 copepods killed per day in a prey field of 282.09 ± 164.82 no. m^{-3} non-*C. anglicus* species. This maybe a generalized and overly simplistic illustration of the potential impacts this range shift could have but highlights the importance of further research and monitoring of zooplankton through long-term monitoring programs.

Funding

The research described in this paper was supported by the Exxon Valdez Oil Spill Trustee Council [project number: 17120114-J]. However, the results and conclusions presented by the authors are their own and do not necessarily reflect the views or position of the Trustee Council.

Declaration of Competing Interest

The authors declare that they have no known competing financial interests or personal relationships that could have appeared to influence the work reported in this paper.

Acknowledgements:

We would like to thank Steve Baird, Angela Doroff, James Schloemer at KBNERR, and Dominic Hondolero at KBL for their help with field sampling and data processing. Mike Geagel and Hans Pedersen at KBL provided at sea support and vessel operations. We also would like to thank the crew of the ADFG vessel the Pandalus.

Appendix A. Supplementary data

Supplementary data to this article can be found online at https://doi.org/10.1016/j.dsr2.2021.105012.

References

Arimitsu, M., Piatt, J., Hatch, S., Suryan, R.M., Batten, S., Bishop, M.A., Campbell, R.W., Coletti, H., Cushing, D., Gorman, K., Hopcroft, R.R., Kuletz, K.J., Marstellar, C., McKinstry, C., McGowan, D., Moran, J., Pegau, S.W., Shaefer, A., Schoen, S., Straley, J., von Biela, V.R., 2021. Heatwave-induced synchrony within forage fish portfolio disrupts energy flow to top pelagic predators. Global Change Biol. 27, 1859–1878.

Ashlock, L., Garcia-Reyes, M., Gentemann, C., Batten, S., Sydeman, W., 2021. Temperature and patterns of occurrence and abundance of key copepod taxa in the Northeast Pacific. Front. Mar. Sci. 8, 670795.

Bakker, J.D., 2008. Increasing the utility of indicator species analysis. J. Appl. Ecol. 45, 1829–1835.

Barbeaux, S., Aydin, K., Fissel, B., Holsman, K., Laurel, B., Palsson, W., Rogers, L., Shotwell, K., Yang, Q., Zador, S., 2019. Chapter 2: assessment of the pacific cod stock in the Gulf of Alaska. North Pacific Fish Manag. Counc. Gulf Alaska Stock Assess. Fish Eval. Rep. 140, 2019. https://archive.afsc.noaa.gov/refm/docs/2019/GOApcod.pdf.

Batten, S.D., Walne, A.W., 2011. Variability in northwards extension of warm water copepods in the NE Pacific. J. Plankton Res. 33, 1643–1653.

Batten, S.D., Raitsos, D.E., Danielson, S., Hopcroft, R., Coyle, K., McQuatters-Gollop, A., 2018. Interannual variability in lower trophic levels on the Alaskan Shelf. Deep-Sea Res. II 147, 58–68.

Bond, N.A., Cronin, M.F., Freeland, H., Mantua, N., 2015. Causes and impacts of the 2014 warm anomaly in the NE Pacific. Geophys. Res. Lett. 42, 3414–3420.

Brodeur, R., Perry, I., Boldt, J., Flostrand, L., Galbraith, M., King, J., Murphy, J., Sakuma, K., Thompson, A., 2017. An Unusual Gelatinous Plankton Event in the NE Pacific: the Great Pyrosome Bloom of, 26. North Pacific Marine Science Organization, pp. 22–27. PICES Press.

Campbell, R.W., 2018. Hydrographic trends in Prince William Sound. Alaska 1960–2016. https://doi.org/10.1016/j.dsr2.2017.08.014. Deep-Sea Res.

Campbell, R.G., Wagner, M.M., Teegarden, G.J., Boudrea, C.A., Durbin, E.G., 2001. Growth and development rates of the copepod *Calanus finmarchicus* reared in the laboratory. Mar. Ecol. Prog. Ser. 221, 161–183.

Clarke, K.R., Ainsworth, M., 1993. A method of linking multivariate community structure to environmental variables. Mar. Ecol. Prog. Ser. 92, 205–219.

Coyle, K.O., Pinchuk, A.I., 2005. Seasonal cross-shelf distribution of major zooplankton taxa on the northern Gulf of Alaska shelf relative to water mass properties, species depth preferences and vertical migration behavior. Deep-Sea Res. II. 52, 217–245.

De Caceres, M., Legendre, P., 2009. Associations between species and groups of sites: indices and statistical inference. Ecology 90, 3566–3574.

Digby, P.S.B., 1950. The biology of the small planktonic copepods of Plymouth. J. Mar. Bio. Assoc. UK. 29, 393–438.

Doroff, A., Campbell, R., McKinstry, C., 2016. Zooplankton Assemblages in Lower Cook Inlet and Kachemak Bay 2012-2014. Alaska Marine Science Symposium. Anchorage, AK, USA.

Dufrene, M., Legendre, P., 1997. Species assemblages and indicator species: the need for a flexible asymmetrical approach. Ecol. Monogr. 67, 345–366.

Environment and Natural Resources Institute (ENRI), 1995. Current water Quality in Cook Inlet, Alaska, Study, 95–0009. OCS Study MMS, Anchorage.

Evans, R., Lea, M.-A., Hindell, M.A., Swadling, K.M., 2020. Significant shifts in coastal zooplankton populations through the 2015/16 Tasman Sea marine heatwave. Estuar. Coast Shelf Sci. 235, 1–11.

Fisher, J., Kimmel, D., Ross, T., Batten, S., Bjorkstedt, E., Galbraith, M., Jacobson, K., Keister, J., Sastri, A., Suchy, K., Zeman, Perry, R.I., 2020. Copepod Responses to, and Recovery from, the Recent Marine Heatwave in the Northeast Pacific, 28. PICES Press, pp. 65–71.

Gibson, V.R., Grice, G.D., 1978. The developmental stages of a species of Corycaeus (copepoda: cyclopoida) from Saanich inlet, British Columbia. Can. J. Zool. 56, 66–74.

Hipfner, J.M., Galbraith, M., Bertram, D.F., Green, D.J., 2020. Basin-scale oceanographic processes, zooplankton community structure, and diet and reproduction of a sentinel North Pacific seabird over a 22-year period. Prog. Oceanogr. 182, 1–11.

Huntley, M., Brooks, E.R., 1982. Effects of age and food availability on diel vertical migration of *Calanus pacificus*. Mar. Biol. (Berl.) 71, 23–31.

Johnson, M.A., 2021. Subtidal surface circulation in lower Cook inlet and Kachemak bay, Alaska. Reg. Stud. Mar. Sci. 41, 1–12.

Keister, J.E., Peterson, W.T., 2003. Zonal and seasonal variations in zooplankton community structure off the central Oregon coast, 1998-2000. Prog. Oceanogr. 57, 341–361.

Keister, J.E., Di Lorenzo, E., Morgan, C.A., Combes, V., Peterson, W.T., 2011. Zooplankton species composition is linked to ocean transport in the Northern California Current. Global Change Biol. 17, 2498–2511.

Landry, M.R., Lehner-Fournier, J.M., Fagerness, V.L., 1985. Predatory feeding behavior of the marine cyclopoid copepod *Corycaeus anglicus*. Mar. Biol. (Berl.) 85, 163–169.

Liang, D., Uye, S., 1996. Population dynamics and production of the planktonic copepods in a eutrophic inlet of the Inland Sea of Japan. III. *Paracalanus* sp. Mar. Biol. (Berl.) 127, 219–227.

Manley, B.F.J., 1994. Multivariate Statistical Methods, second ed. Chapman & Hall, London, p. 215.

McKinstry, C.A.E., Campbell, R.W., 2018. Seasonal variation of zooplankton abundance and community structure in Prince William Sound, Alaska. Deep-Sea Res. Part II 47, 69–78, 2009–2016.

Morgan, C.A., Peterson, W.T., Emmett, R.L., 2003. Onshore-offshore variations in copepod community structure off the Oregon coast during the summer upwelling season. Mar. Ecol. Prog. Ser. 249, 223–236.

Musgrave, D.L., Halverson, M.J., Pegau, W.S., 2013. Seasonal surface circulation, temperature, and salinity in Prince William Sound, Alaska. Continent. Shelf Res. 53, 20–29.

Okkonen, S., Pegau, S., Saupe, S., 2009. Seasonality of Boundary Conditions for Cook Inlet, Alaska. Final Report OSC Study MMS 2009-041. Coastal Marine Institute, University of Alaska Fairbanks.

Oksanen, J., Blanchet, F.G., Friendly, M., Kindt, R., Legendre, P., McGlinn, D., Minchin, P.R., O'Hara, R.B., Simpson, G.L., Solymos, P., Stevens, M.H.H., Szoecs, E., Wagner, H., 2019. vegan: community Ecology Package. R package version 2.5-6. https://CRAN.R-project.org/package=vegan.

Perry, R.I., King, S., Boldt, J., Chandler, P., 2017. Unusual events in Canada's Pacific marine waters in 2016. Can. Tech. Rep. Fish. Aquat. Sci.. In: Chandler, P., King, S., Boldt, J. (Eds.), State of the Physical, biological and Selected Fishery Resources of Pacific Canadian Marine Ecosystems in 2016, 3225, p. 243 (+ vi p).

Peterson, W.T., Keister, J.E., 2003. Interannual variability in copepod community composition at a coastal station in the northern California Current: a multivariate approach. Deep-Sea Res. II 50, 2499–2517.

Peterson, W.T., Fisher, J.L., Strub, P.T., Du, X., Risien, C., Peterson, J., Shaw, C.T., 2017. The pelagic ecosystem in the Northern California Current off Oregon during the 2014–2016 warm anomalies within the context of the past 20 years. J. Geophys. Res. Oceans 122, 7267–7290.

Piatt, J.F., Parrish, J.K., Renner, H.M., Schoen, S.K., Jones, T.T., Arimitsu, M.L., Kuletz, K.J., Bodenstein, B., Garcia-Reyes, M., Duerr, R.S., Corcoran, R.M., Kaler, R. S.A., McChesney, G.J., Golightly, R.T., Coletti, H.A., Suryan, R.M., Burgess, H.K., Lindsey, J., Lindquist, K., Warzybok, P.M., Jahncke, J., Roletto, J., Sydeman, W.J., 2020. Extreme mortality and reproductive failure of common murres resulting from the northeast Pacific marine heatwave of 2014-2016. PLOS ONE 15, 1–32.

R Core Team, 2019. R: A Language and Environment for Statistical Computing. R Foundation for Statistical Computing, Vienna, Austria. URL: https://www.R-project.org/.

Runge, J.A., Ji, R., Thompson, C.R.S., Record, N.R., Chen, C., Vandemark, D.C., Salisbury, J.E., Maps, F., 2015. Persistence of *Calanus finmarchicus* in the western Gulf of Maine during recent extreme warming. J. Plankton Res. 37, 221–232.

Savage, K., 2017. Alaska and British Columbia Large Whale Unusual Mortality Event Summary Report. NOAA Affiliate Protected Resources Division, NOAA Fisheries Juneau, AK. August 17 2017. https://repository.library.noaa.gov/view/noaa/17715.

Sousa, L., Coyle, K.O., Barry, R.P., Weingartner, T.J., Hopcroft, R.R., 2016. Climate-related variability in abundance of mesozooplankton in the northern Gulf of Alaska 1998–2009. Deep-Sea Res. II 132, 122–135.

Suryan, R.M., Arimitsu, M.L., Coletti, H.A., Hopcroft, R.R., Lindeberg, M.R., et al., 2021. Ecosystem response persists after a prolonged marine heatwave. Sci. Rep. 11, 6235.

Vandersea, M.W., Kibler, S.R., Tester, P.A., Holderied, K., Hondolero, D.E., Powell, K., Baird, S., Doroff, A., Dugan, D., Litaker, R.W., 2018. Environmental factors influencing the distribution and abundance of *Alexandrium catenella* in Kachemak Bay and lower Cook Inlet, Alaska. Harmful Algae 77, 81–92.

von Biela, V.R., Arimitsu, M.L., Piatt, J.F., Heflin, B., Schoen, S.K., Trowbridge, J.L., Clawson, C.M., 2019. Extreme reduction in nutritional value of a key forage fish during the Pacific marine heatwave of 2014-2013. Mar. Ecol. Prog. Ser. 613, 171–182.

Wood, S.N., 2004. Stable and efficient multiple smoothing parameter estimation for generalized additive models. J. Am. Stat. Asses. 99, 673–686.